JOURNAL OF BACTERIOLOGY, Feb. 2009, p. 754–761 Vol. 191, No. 3
0021-9193/09/$08.00+0 doi:10.1128/JB.01439-08

The MalF P2 Loop of the ATP-Binding Cassette Transporter $MalFGK_2$ from *Escherichia coli* and *Salmonella enterica* Serovar Typhimurium Interacts with Maltose Binding Protein (MalE) throughout the Catalytic Cycle▽

Martin L. Daus, Mathias Grote, and Erwin Schneider*

Institut für Biologie, AG Bakterienphysiologie, Humboldt-Universität zu Berlin, Chausseestr. 117, D-10115 Berlin, Germany

Received 14 October 2008/Accepted 20 November 2008

We have investigated the interaction of the uncommonly large periplasmic P2 loop of the MalF subunit of the maltose ATP-binding cassette transporter ($MalFGK_2$) from *Escherichia coli* and *Salmonella enterica* serovar Typhimurium with maltose binding protein (MalE) by site-specific chemical cross-linking in the assembled transport complex. We focused on possible distance changes between two pairs of residues of the P2 loop and MalE during the transport cycle. The distance between MalF(S205C) and MalE(T80C) (~5 Å) remained unchanged under all conditions tested. Cross-linking did not affect the ATPase activity of the complex. The distance between MalF(T177C) and MalE(T31C) changed from ~10 Å to ~5 Å upon binding of ATP (or maltose, with a less pronounced result) and was reset to ~10 Å after hydrolysis of one ATP. A cross-link (~25 Å) between MalF(S205C) and MalE(T31C) was observed only when the transporter resided in a transition state-like conformation, as was the case after vanadate trapping or in a binding protein-independent mutant, both of which are characterized by tight binding of unliganded MalE to the transporter. Thus, we propose that the observed cross-link is indicative of catalytic intermediates of the transporter. Together, our results strengthen the notion that the MalF P2 loop plays an important role in intersubunit communication. In particular, this loop is involved in keeping MalE in close contact with the transporter. The data are discussed with respect to a crystal structure and current transport models.

ATP-binding cassette (ABC) transporters utilize the free energy of ATP hydrolysis to translocate substrates across biological membranes and can function as import or export systems (17). ABC transporters are generally composed of two hydrophobic, pore-forming transmembrane subunits and transmembrane domains (TMDs) and two hydrophilic nucleotide-binding (or ABC) subunits and nucleotide-binding domains (NBDs) that hydrolyze ATP (9). The crystal structures of isolated NBDs (6, 23, 34, 43) revealed that NBDs can be divided into a RecA-like subdomain comprising both the Walker A and the Walker B motifs, which are involved in nucleotide binding, and a helical subdomain harboring the unique LSGGQ motif (35). Furthermore, in the physiologically relevant NBD dimer, the nucleotide is complexed between the Walker A and B sites of one monomer and the LSGGQ motif of the opposing monomer. Both subdomains are joined by the "Q loop" containing a conserved glutamine residue that binds to the Mg^{2+} ion and attacking water and is likely to be involved in communicating ATP binding to the TMDs (10, 20, 29). ATP-dependent closing of the NBD dimer is thought to provide one possibility of the power stroke of ABC transporters (38).

ABC importers that are confined to prokaryotes mediate the uptake of a large variety of solutes, including inorganic ions, amino acids, sugars, vitamins, oligopeptides, and polyamines (5). They require an additional protein, the extracytoplasmic solute binding protein (SBP), in order to capture the substrate and to deliver it to the cognate ABC transporter (37). SBPs typically consist of two lobes that are connected by a linker region. The interface between the two lobes forms the substrate binding site. Upon binding of the ligand, the proteins undergo a conformational change from an open toward a closed state (33) which, by interaction with extracytoplasmic peptide regions of TMDs of the cognate ABC transporter, initiates the transport process (31). The molecular events by which binding of ATP to the NBDs and interaction of liganded binding proteins with the TMDs are communicated to eventually trigger substrate translocation are still poorly understood.

The maltose ABC transporter of *Escherichia coli* and *Salmonella enterica* serovar Typhimurium is one of the best-characterized transporters and thus serves as a model system for studying the mechanism by which ABC transporters exert their functions in general (15). The transporter is composed of the extracytoplasmic (periplasmic) maltose binding protein (MalE), the membrane-spanning subunits MalF and MalG, and two copies of the ATP-hydrolyzing subunit (MalK) (Fig. 1A).

Recently, suppressor mutational analysis provided a first hint that substrate availability is communicated from MalE to the MalK dimer via periplasmic loop regions of MalFG (11). Moreover, by site-directed cross-linking based on previous genetic evidence (19, 40), we demonstrated a close proximity of MalE G13 to Pro-78 in the first periplasmic loop (P1) of MalG, independently of cofactors such as maltose or ATP. Interaction of both residues was also observed in intact cells (11).

* Corresponding author. Mailing address: Humboldt-Universität zu Berlin, Institut für Biologie, AG Bakterienphysiologie, Chausseestr. 117, D-10115 Berlin, Germany. Phone: 49(0)30-20938121. Fax: 49(0)30-20938126. E-mail: erwin.schneider@rz.hu-berlin.de.

▽ Published ahead of print on 1 December 2008.

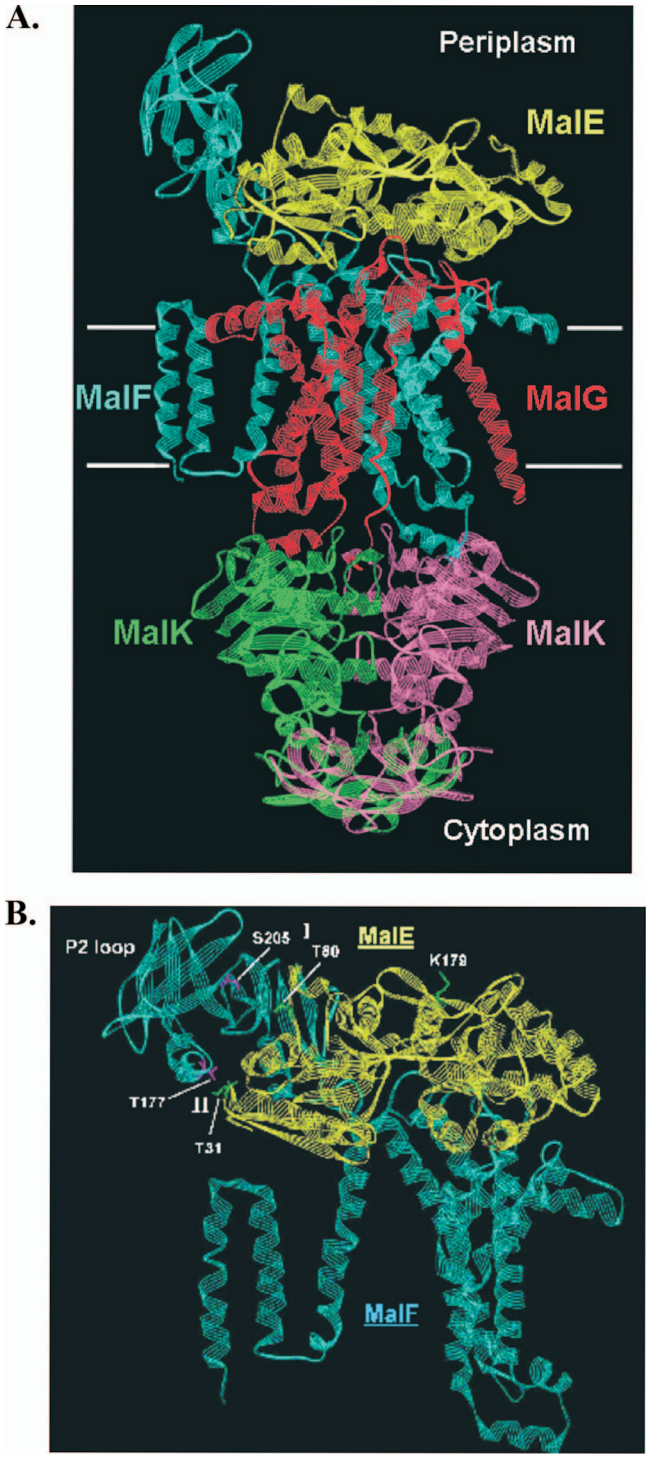

FIG. 1. (A) Structure of the catalytic intermediate of the maltose transporter [MalFGK(E159Q)$_2$-E]. The complex is shown in a ribbon diagram. White horizontal bars mark the boundaries of the membrane. Color code: yellow, MalE; cyan, MalF; red, MalG; green and magenta, MalK dimer. (B) Close-up view of the contact site between MalF P2 and the N-terminal lobe of MalE. The color code is the same as that for panel A. Residues from regions I and II that were replaced by cysteines are indicated in pink (MalF) and green (MalE). Residue MalE-K179, which was used as a control, is shown in green. The figure was drawn with DS ViewerPro 6.0 (Accelrys, Cambridge, United Kingdom), using the coordinates from entry 2R6G in the Brookhaven Protein Data Bank.

These findings led us to propose that a copy of MalE is permanently associated with the transporter throughout the catalytic cycle. Furthermore, we have found that a region of the large, periplasmic P2 loop of MalF around Ser-205 (Fig. 1) is in cross-linking distance from MalE in the presence of maltose and MgATP only or when the transporter resides in the vanadate-trapped transition state. These results were perfectly confirmed by the subsequently published crystal structure of the MalFGK(E159Q)$_2$-E complex, which represents a transport intermediate (32). Here, the MalK dimer is complexed with two ATP molecules, and MalE is tightly associated with MalFG, but maltose has already been released into a binding pocket formed by MalF only. In particular, the N-terminal lobe of MalE is in close contact with the P2 loop of MalF (Fig. 1A).

In this communication, we have taken advantage of this structural information to gain further insight into the MalF P2-MalE interaction during the transport cycle. We demonstrate ATP- and maltose-dependent distance changes between selected pairs of residues of the loop and MalE in the assembled complex by site-specific cross-linking. Our data demonstrate for the first time that the MalF P2 loop is in close contact to MalE throughout the catalytic cycle.

MATERIALS AND METHODS

Bacterial strains, plasmids, and media. *E. coli* strain JM109 (Stratagene) served as a host for the plasmids listed in Table 1. The plasmid-borne *malK* alleles originated from the *Salmonella enterica* subsp. *enterica* serovar, whereas the *malF malG malE* alleles were from *E. coli*. The *mal* genes from both organisms are functionally fully exchangeable (20). Bacteria were usually grown in LB (28) or TP$_i$ (21) medium, supplemented with ampicillin (100 μg ml^{-1}) and/or chloramphenicol (20 μg ml^{-1}) if required.

Construction of plasmids and mutagenesis. Cysteine residues replacing MalF T177, MalE T31, MalE T80, and MalE K179 were introduced by Stratagene's QuikChange kit, using the plasmids pTAZFGQ* [*malF*(Cys$^-$) *malG*(Cys$^-$)] (20) and pMM20 (10) as templates for *malF* and *malF500*, respectively, and pCB6 (11) as a template for *malE*. The resulting plasmids are listed in Table 1.

Purification of MalFGK$_2$ complexes. Polyhistidine-tagged transport complex variants harboring the plasmids pBB01 (wild-type complex), pMM56/pMM37 [MalF*(T177C) MalG* MalK(C40S)$_2$], pMM26/pMM37 [MalF*(S205C) MalG* MalK(C40S)$_2$], pMM59/pMM37 [MalF500*(S205C) MalG* MalK(C40S)$_2$], and pMM62/pMM37 [MalF500*(T177C) MalG* MalK(C40S)$_2$] were overproduced in strain JM109. Purification was essentially carried out as described in reference 21. Briefly, proteins solubilized from membrane vesicles by addition of 1.1% dodecyl-β-D-maltoside (DDM) were bound to nitrilotriacetic acid resin equilibrated in buffer A (50 mM Tris-HCl, pH 7.5, 5 mM $MgCl_2$, 20% glycerol, 0.1 mM phenylmethylsulfonyl fluoride [PMSF], 0.01% DDM). The resin was washed with buffer B (20 mM imidazole, 50 mM Tris-HCl, pH 7.5, 5 mM $MgCl_2$, 20% glycerol, 0.1 mM PMSF, 0.01% DDM), and protein was eluted with buffer C (100 mM imidazole, 50 mM Tris-HCl, pH 7.5, 5 mM $MgCl_2$, 20% glycerol, 0.1 mM PMSF, 0.01% DDM). Peak fractions were pooled, passed through a PD10 column (GE Healthcare) equilibrated with buffer D (50 mM Tris-HCl, pH 7.5, 20% glycerol, 0.01% DDM), concentrated by ultrafiltration, shock frozen in liquid nitrogen, and stored at −80°C. All preparations displayed MalE/maltose-stimulated ATPase activities similar to that of the wild type (~0.5 μmol phosphate min^{-1} mg^{-1}) and consistent with previous reports (11, 21). Binding protein-independent variants exhibited ATPase activities of ~0.8 μmol phosphate min^{-1} mg^{-1}, regardless of the presence or absence of MalE/maltose (10).

Purification of MalE. Polyhistidine-tagged MalE variants harboring plasmids pCB6 (wild type), pMM55 (T31C), pMM47 (K179C), and pMM60 (T80C) were overproduced in strain JM109. Purification was carried out as described in reference 11.

Vanadate trapping. Vanadate-trapped complexes were prepared as described in reference 10.

Cross-linking. Cross-linking experiments using Cu(1,10-phenanthroline)$_2$SO$_4$ or homobifunctional sulfonate linkers were performed as described in reference 10. Sulfonate cross-linkers were purchased from Toronto Chemicals (Toronto, Canada). The following cross-linkers were used: 1,2 ethanediyl-bismethanethio-

TABLE 1. Plasmids used in this study

Plasmid	Relevant genotype or description[a]	Source or reference
pQE9	Ap^r; p_{T5}; His_6-coding sequence (5′)	Qiagen
pSU19	LacZα; Rep(p15A); Cm^r	26
pTZ18R	Phagemid; P_{tac}	GE Healthcare
pTAZFGQ(F*G*)	*E. coli malF*(Cys^-) *malG*(Cys^-) on pTZ18R	20
pBB1	p_{T5} $malK_{ht}$; p_{tre} *malF malG* Ap^r on pQE9	21
pMM20	*E. coli malF*(*G338R*/*N505I*) (Cys^-) *malG*(Cys^-) on pTZ18R [derivative of pTAZFGQ(F*G*)]	10
pMM26	*E. coli malF*(*S205C*) *malG*(Cys^-) on pTZ18R [derivative of pTAZFGQ(F*G*)]	11
pMM37	p_{T5} $malK796_{ht}$ (His_6-C40S) on pSU19	12
pMM47	$malE_{ht}$(*K179C*) on pQE9 (derivative of PCB6)	This study
pMM55	*malEht*(*T31C*) on pQE9 (derivative of pCB6)	This study
pMM56	*E. coli malF*(*T177C*) *malG*(Cys^-) on pTZ18R [derivative of pTAZFGQ(F*G*)]	This study
pMM59	*E. coli malF*(*G338R*/*N505I*/*S205C*) *malG*(Cys^-) on pTZ18R (derivative of pMM20)	This study
pMM60	$malE_{ht}$(T80) on pQE9 (derivative of pCB6)	This study
pMM62	*E. coli malF*(*G338R*/*N505I*/*T177C*) *malG*(Cys^-) on pTZ18R (derivative of pMM20)	This study

[a] ht, His tag.

sulfonate (EBS), 1,6 hexandiyl-bismethanethiosulfonate (HBS), and 3,6,9,12,15-pentaoxaheptadecan-1,17-diyl-bis-methanethiosulfonate (PBS). The approximate spacer lengths are 5.2 Å (EBS), 10.4 Å (HBS), and 24.7 Å (PBS) (22). Reactions were started by adding the respective cross-linker (final concentration, 1 mM) from freshly prepared stock solutions (100 mM in dimethyl sulfoxide) to the indicated protein samples (2.5 μM $MalFGK_2$ variants and 5 μM MalE variants) in 50 mM Tris-HCl, pH 7.5, 20% glycerol, 0.01% DDM (buffer D). After 20 min at room temperature, reactions were terminated by adding 5 mM *N*-ethylmaleimide.

Analytical procedures. ATPase assays, sodium dodecyl sulfate-polyacrylamide gel electrophoresis (SDS-PAGE), and immunoblotting were performed as described in reference 12. Protein concentrations were routinely determined as described in reference 10.

RESULTS

Rationale of the study and experimental system. In our previous work, we demonstrated a close contact between the P2 loop regions of MalF and MalE (11). In particular, we found that the purified transport complex MalF*(S205C) MalG* $MalK(C40S)_2$ (* denotes a Cys-less background) can be cross-linked with MalE by the heterobifunctional photolabile cross-linker benzophenone-4-maleimide in the presence of maltose and MgATP or after treatment with vanadate only. Vanadate locks the transporter in a transition-like state by preventing dissociation of ADP after hydrolysis of one ATP molecule. Under these conditions, MalE can be copurified with the transport complex, indicating a tight association (7). Our results suggested that the P2 loop might undergo a conformational change during the transport cycle. However, analysis of the cross-linked product by mass spectrometry failed to identify the position of the photo-cross-link in MalE. Nonetheless, our findings were subsequently supported by the crystal structure of the $MalFGK(E159Q)_2$-E complex (32).

Now, with the structure at hand, we addressed the question of whether the MalF P2 loop is constantly or only transiently in close contact with MalE. To this end, we performed cross-linking experiments with two pairs of residues selected from two opposite regions (designated I and II) of the contact site between MalF P2 and the N-terminal lobe of MalE in the crystal structure (Fig. 1B). Accordingly, Thr-177 and Ser-205 of MalF P2 are in close proximity to Thr-31 and Thr-80 of MalE, respectively. These residues were consequently replaced by cysteines by site-directed mutagenesis, and cross-linking experiments were performed with purified complex variants in detergent solution. As demonstrated by ATPase assays, both transporter variants displayed MalE/maltose-stimulated ATPase activities comparable to that of the wild type. Furthermore, the MalE(T31C) and MalE(T80C) variants stimulated ATP hydrolysis of wild-type and mutant $MalFGK_2$ complexes, like native MalE (not shown, but see Materials and Methods).

Cross-linking experiments were performed under different conditions mimicking several states of the transporter: (i) the apo state (absence of cofactors), (ii) the ATP- and/or maltose-bound state, (iii) the posthydrolysis state, and (iv) the vanadate-trapped transition state. As in our previous study (10), homobifunctional sulfonate linkers with spacer lengths of ~5 Å (EBS), ~10 Å (HBS), and ~25 Å (PBS) were applied.

Cross-linking of residues MalF(S205C) and MalE(T80C) from region I. First, we analyzed possible distance changes between MalF S205 and MalE T80 by using the respective complex variant [MalF*(S205C) MalG* $MalK(C40S)_2$]. As shown in Fig. 2A, in the apo state, a MalF-MalE cross-link product identified by immunoblotting (Fig. 2B) was formed with EBS, suggesting that the distance between the two residues can be as short as 5 Å. This result is in good agreement with the Cβ-Cβ distance determined from the X-ray structure of the complex intermediate (8.6 Å) (32). Addition of maltose, ATP, or $MgCl_2$ (to initiate ATP hydrolysis) or vanadate trapping of the complex prior to cross-linking resulted in a similar pattern (Fig. 2A). The specificities of these and all subsequent cross-linking reactions were verified by replacing the respective MalE mutants with the MalE variant K179C. This residue is located in the hinge region of MalE (Fig. 1B) and, according to the crystal structure, not in cross-linking distance to the MalF variants considered in this study. As expected, no cross-linked products were obtained under any of the conditions applied above (Fig. 2A).

The rather significant yield of cross-link product that was formed under the above-mentioned conditions (Fig. 2A [please note the decrease in MalF compared to MalFGK alone]) prompted us to investigate whether covalent linkage between

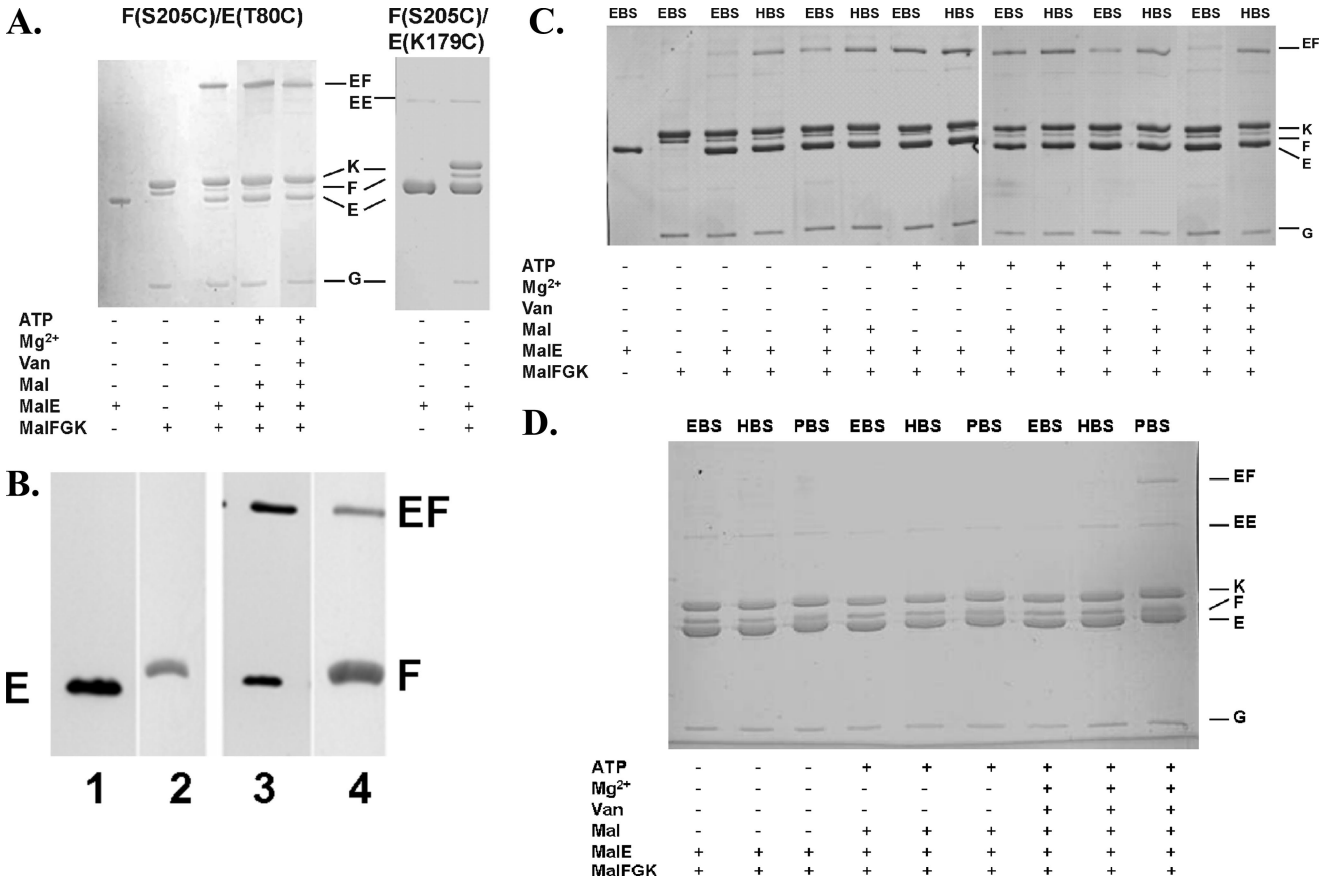

FIG. 2. Site-specific cross-linking between MalF P2 residues and MalE variants. Purified cysteine variants of the transport complex (2.5 μM) and MalE (5 μM) were incubated with homobifunctional sulfonate cross-linkers as indicated in the presence of different cofactors, as described in Materials and Methods, and subsequently analyzed by SDS-PAGE. (A) Cross-linking of MalF*(S205C) G*K(C40S)$_2$ with MalE(T80C) in the presence of EBS. (B) Immunoblot analysis of reaction mixtures from panel A probed with antisera raised against MalE (lanes 1 and 3) and MalF (lanes 2 and 4). Lanes: 1, MalE(T80C); 2, MalF*(S205C) G*K(C40S)$_2$; 3 and 4, MalF*(S205C) G*K(C40S)$_2$ and MalE(T80C). All samples contained EBS. (C) Cross-linking of MalF*(T177C) G*K(C40S)$_2$ with MalE(T31C). (D) Cross-linking of MalF*(S205C) G*K(C40S)$_2$ with MalE(T31C). Van, vanadate; Mal, maltose.

MalF(S205C) and MalE(T80C) would affect the ATPase activity of the transporter. To this end, the respective complex and MalE variants were incubated with Cu(1,10-phenanthroline)$_2$SO$_4$ to induce a disulfide bond between the two cysteine residues. Although the efficiency of cross-linking was similar to that of the sulfonate linkers, as demonstrated by SDS-PAGE (not shown), ATPase activity remained unaffected.

Together, these results lead us to conclude that MalF S205 and MalE T80 do not change their positions relative to each other during transport.

Cross-linking of residues MalF(T177C) and MalE(T31C) from region II. Next, we studied distance changes between engineered cysteines at positions 177 and 31 of MalF and MalE, respectively. As shown in Fig. 2C, in the apo state, a strong cross-link product containing MalF and MalE was formed with HBS while only a very faint band was seen with EBS, suggesting an approximate distance of 10 Å between MalF(T177C) and MalE(T31C) in the majority of transport complexes. In contrast, in the presence of ATP, the distance is reduced to ~5 Å, in agreement with the crystal structure. Strikingly, this conformational change occurs independently of the substrate, although maltose, in the absence of ATP, also induces a cross-link with EBS, but it is less pronounced. Adding maltose to the ATP-bound state, however does not change the yield in cross-link product compared to the level for ATP alone. The addition of Mg^{2+} ions to initiate hydrolysis of ATP resulted in a preferred cross-linking product at a distance of ~10 Å, resembling the pattern obtained in the presence of maltose alone. This finding clearly indicates that hydrolysis resets the P2 loop in the apo state. The presence of ADP and/or rebinding of maltose to MalE under the experimental conditions applied might account for residual cross-link product at ~5 Å. The above conclusion is further corroborated by the cross-linking results obtained with the vanadate-trapped transporter. Here, the distance between the two residues was found almost only to be around 10 Å. Apparently, the two residues move apart after only one step of ATP hydrolysis.

MalF(S205C) can be cross-linked to MalE(T31C) in transport intermediates only. Finally, we investigated possible distance changes between residues from both regions of the MalF-MalE contact site (Fig. 1B). To this end, cross-linking experiments were performed with MalF*(S205C) G*K(C40S)$_2$ and MalE(T31C). We were able to detect a cross-link product only under vanadate-trapped conditions when using a 25 Å

cross-linker (PBS) (Fig. 2D). Since a cross-link product was not observed with HBS, the distance between the two residues is likely to be in the range of >10 to 25 Å. This finding is perfectly in line with the idea that the crystal structure represents a catalytic intermediate that proposes a distance (Cβ-Cβ) of 21 Å between the two residues (32).

Interestingly enough, binding of ATP to the (crystallized) MalFGK(E159Q)$_2$-E mutant transporter and vanadate trapping of wild-type MalFGK$_2$ each cause formation of a tight and stable complex with MalE that can be isolated by gel filtration (24, 32). Thus, the above-mentioned result tempted us to speculate that the distance change between MalF(S205C) and MalE(T31C) might be indicative of this feature. To further prove this notion, we performed cross-linking with a binding protein-independent maltose transport complex, representing yet another type of mutant that is considered to reside in a transition state-like conformation (10, 12, 13, 24, 36). Several such complex variants exist, most of which carry two mutations in the transmembrane segments of MalF or MalG (8). These variants exhibit spontaneous ATPase activity, transport maltose with a significantly higher K_m than the wild type, and, strikingly, also form a tight complex with MalE (13, 36). In this study, we considered variant MalF500, which carries mutations affecting G338R and N505I (8). Consequently, both mutations were introduced into MalF*(S205C) G*K(C40S)$_2$, and the resulting complex variant was purified from the respective overproducing strain (Table 1). The binding protein-independent phenotype was verified by assaying ATPase activity in the absence of MalE (see also references 10 and 12).

In Fig. 3A, the results of cross-linking experiments are shown. As in the wild-type background, a MalF-MalE product was formed with PBS under vanadate-trapped conditions, but in contrast to the data shown in Fig. 2D, the cross-link was also found in the apo state (Fig. 3A) and in the presence of ATP or maltose (not shown). Thus, these findings are perfectly in line with the above-mentioned notion.

In the binding protein-independent mutant, the distance between MalF(T177C) and MalE(T31C) is arrested at ~10 Å. Having proven that MalF500 provides a useful tool in order to evaluate cross-linking data obtained with the wild-type complex, we also introduced both mutations that cause a binding protein-independent phenotype into MalF*(T177C) G*K(C40S)$_2$. As demonstrated above (Fig. 2C), residue T177 of MalF and T31 of MalE approach each other upon ATP binding but move apart after ATP hydrolysis and under vanadate-trapped conditions, which requires one step of hydrolysis. Once again, if the transition state-like conformation of the binding protein-independent mutant resembles that of the vanadate-trapped state, a cross-link product should be observed with HBS only. Figure 3B shows that this is indeed true.

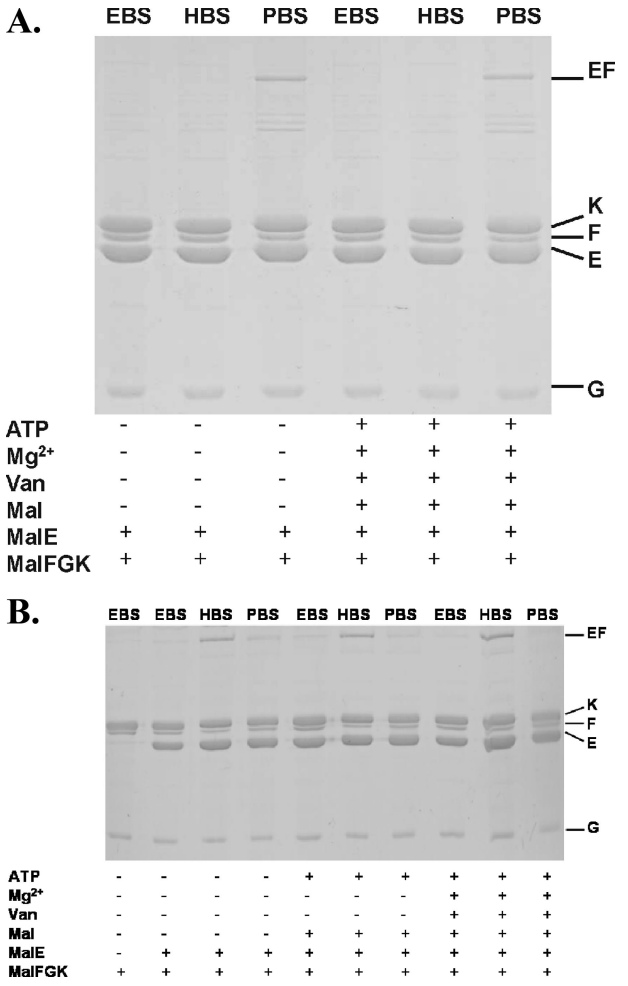

FIG. 3. Site-specific cross-linking of binding protein-independent mutants with MalE(T31C). (A) MalF500*(S205C) G*K(C40S)$_2$. (B) MalF500*(T177C) G*K(C40S)$_2$. See the legend to Fig. 2 for further details.

DISCUSSION

In this study, we show for the first time that the unusually large MalF P2 loop is in close contact with maltose binding protein during the transport cycle. Moreover, we provide direct evidence for changes in the interaction patterns of MalF P2 and MalE.

ATP hydrolysis by the transporter is thought to be triggered by the interaction of liganded MalE and the transmembrane proteins (13). How substrate availability in the periplasmic space is signaled to the cytosolic ABC subunits to induce ATP hydrolysis is still highly speculative. In our previous work, we found a first clue to this question by studying suppressor mutations of a complex variant that carries a mutation (Q140K) near the signature sequence (**LSGGQ**RQ$_{140}$) (highly conserved residues are shown in bold) of MalK (11). Three out of four suppressor mutations were located in periplasmic loop regions of MalFG and could partially restore the transport activity that was highly reduced by the mutated signature sequence. On the basis of these results and subsequent cross-linking data, we speculated that substrate-loaded binding protein leads to conformational changes in periplasmic loop regions that transmit these conformational changes to the MalK subunits, thereby inducing ATP hydrolysis (11).

To gain further insight into these interactions, we have focused on the P2 loop of MalF, as it is unusually large and, according to the crystal structure of the complete transporter (32), at least transiently in close contact with the N-terminal lobe of MalE. The MalF P2 loop seems to be confined to enteric bacteria and a few close relatives. Insertions or dele-

TABLE 2. Distances between selected residues in MalF and MalE as determined by cross-linking and Cβ-Cβ distances from the X-ray structure of the maltose ABC transporter

Residues in MalF/MalE	Distance (Å) between residues in:				
	MalFGK $(E159Q)_2$-E (Cβ-Cβ)[a]	MalF500	Wild type in indicated state		
			ATP-bound	Apo or posthydrolysis	Vanadate-trapped
S205C/T80C	8.6	ND[b]	~5	~5	~5
T177C/T31C	5	>5–10	~5	>5–10	>5–10
S205C/T31C	21	>10–25	>25	>25	>10–25

[a] Determined from the X-ray structure (Protein Data Bank number 2R6G) with DS ViewerPro 6.0 (Accelrys, Cambridge, United Kingdom).
[b] ND, not determined.

tions in this region are often not tolerated with respect to transport function (42). Two pairs of residues from two opposite regions of the contact site between MalF P2 and MalE (Fig. 1B) were chosen to study motional changes during the transport cycle by site-specific chemical cross-linking. Our results can be summarized as follows (Table 2).

(i) The distance between residues MalF(S205C) and MalE (T80C) from region I remained unchanged under all conditions tested (Fig. 2), suggesting that no larger conformational changes of the polypeptide chains occur in this region. This notion is supported by the observation that cross-linking of both residues did not affect the ATPase activity of the complex.

(ii) The distance between residues MalF(T177C) and MalE(T31C) from region II changes from ~10 Å in the apo state to ~5 Å upon binding of ATP (or maltose, but less efficiently), as in the crystal structure (32), but is reset to ~10 Å after hydrolysis of one ATP (as seen under vanadate-trapped conditions) (Fig. 2D). These findings are corroborated by results obtained with a binding protein-independent mutant thought to reside in a transition state-like conformation (Fig. 3B).

(iii) A cross-link (~25 Å) between MalF(S205C) from region I and MalE(T31C) from region II is observed only when the transporter resides in a transition state-like conformation, as in the crystallized mutant MalFGK$(E159Q)_2$-E (32), in the vanadate-trapped complex (Fig. 2D) or in a binding protein-independent variant (Fig. 3A). This finding is particularly intriguing, as in all three cases, MalE is in its open conformation (2, 7, 32) and MalK is present as a closed (ATP-bound) dimer (10, 16). However, in the vanadate-trapped state, one ATP has already been hydrolyzed (7) whereas the E159Q mutation prevents ATP hydrolysis (10, 12). Since ATP binding was insufficient to induce the formation of a cross-linked product between MalF(S205C) and MalE(T31C) in the wild-type complex (Fig. 2D), its conformation must differ from that of the ATP-bound MalFGK$(E159Q)_2$-E complex.

Furthermore, taking into account that residue MalF S205 is unlikely to undergo motional changes during the transport cycle as discussed above, the distance change observed between S205 and MalE T31 must be attributed mainly to the latter. Indeed, when the closed (substrate-loaded) form of MalE (Protein Data Bank number 1ANF) is modeled into the crystal structure of the maltose transporter, it becomes obvious that residue Thr-31 is positioned ~29 Å (Cβ-Cβ distance) apart from Ser-205. This could explain why a cross-link between the two residues could not be formed with PBS (~25 Å). However, a cross-link was not obtained with unliganded MalE either (Fig. 2D), although in the crystal structure, MalE is in its open conformation and the distance between Ser-205 and Thr-31 within the range of PBS (~21 Å) (Table 2). Thus, the relative positions of unliganded MalE T31 and MalF S205 in the state prior to the addition of maltose must differ from those occurring after the release of maltose. Alternatively, the failure to cross-link the two residues by PBS in the absence of maltose (Fig. 2D) could be due to the presence of an unliganded but closed conformer of MalE, as recently observed by paramagnetic nuclear magnetic resonance (41).

Concerning the absolute numbers given above, a note of caution appears appropriate since cross-linking is highly influenced by side chain dynamics and the molecular surroundings of the target residues. Consequently, distances between two residues might be underestimated (39). However, compared with a different experimental tool, such as site-directed spin-labeling electron paramagnetic resonance spectroscopy, cross-linking results proved to be consistent qualitatively (16, 39). Keeping this restriction in mind, we will nonetheless discuss our results by referring to distances obtained with the sulfonate linkers.

Together, our findings add to the notion that the MalF P2 loop indeed plays an important role in intersubunit communication. In particular, residues involved in contacting MalE in region II rather than those from region I might be crucial in this respect. However, a role for other parts of the P2 loop is likely, as ATP-dependent changes in the local environment of residues Ser-252 and Lys-262 were observed by limited proteolysis and fluorescence spectroscopy (12).

Furthermore, our results, together with previous findings demonstrating a close contact between MalE(G13C) and P78C in the P1 loop of MalG independently of cofactors (11), support a model in which a copy of MalE is associated more or less tightly with the transport complex during all steps of the catalytic cycle. This is in contrast to models that propose a dissociation-association process of SBPs upon substrate release and binding (14) but agrees with results presented for the histidine ABC transporter of *S. enterica* serovar Typhimurium (1) and with the crystal structure of the MalFGK$(E159Q)_2$-E transporter (32). Interactions between MalE and periplasmic loop regions are clearly visible in the structure, in particular for the P3 loop of MalG, which reaches into the binding cleft of MalE, and for the P2 loop of MalF. Insertion of periplasmic loop regions into the binding protein was also found in the structure of Btu$(CD)_2$-F (18). Thus, our results are consistent with the notion that binding of maltose to MalE that is associated with the ATP-loaded transporter triggers hydrolysis of ATP and thereby initiates the transport cycle.

As previously discussed in more detail (11), the concept of a copy of MalE being permanently associated with a transport complex molecule is consistent with earlier findings based on mathematical treatment of transport data, which suggested that both the substrate-loaded and the substrate-free forms of MalE have access to MalFG (4, 27). On the other hand, this seems to be contradicted by the failure to isolate a MalE-MalFGK_2 complex with wild-type proteins in the absence of vanadate, indicating that MalE has a rather low level of affinity for its membrane partner. Indeed, rough estimates from trans-

port assays (~90 μM) (25) and from cross-linking experiments (11) revealed dissociation constants in the micromolar range. Isothermal titration calorimetry performed with isolated MalF P2 (encompassing residues Asn-93 to Lys-275) and MalE resulted in a dissociation constant of 10 to 20 μM (T. Jacso, M. Grote, M. L. Daus, P. Schmieder, S. Keller, E. Schneider, and B. Reif, unpublished results), thereby corroborating the above-mentioned values. However, in the periplasm of an intact *E. coli* cell, there is an observed 30- to 50-fold excess of MalE relative to $MalFGK_2$, 20% of which was found to be necessary for full transport activity (25). Similar findings were reported in cases of other binding proteins from gram-negative bacteria (1). Together, these data at least do not exclude a model of the transport process that involves binding of MalE in all states.

Upon a summary of the results presented in this communication, together with other data, the following transport scenario emerges. A copy of maltose binding protein that may at the initial state constantly exchange with the pool of MalE molecules in the periplasm is in close contact with $MalFGK_2$. Since the cytoplasmic concentration of ATP is at least 1 order of magnitude higher than the K_m of the transporter (3, 30), the ATP-bound form is likely to represent the resting state of the transporter in vivo. The (ATP-bound) MalK dimer resides in a (semi-) open conformation, with the transmembrane proteins open on the cytosolic side and closed on the periplasm (37). At this stage, the upper part of the MalF P2 loop around residue Ser-205 is positioned rather distantly (>25 Å) from MalE T31 (Fig. 2D) while the region around Thr-177 is at a ~5-Å distance from MalE T31 (Fig. 2C). Furthermore, residues MalF S205 and MalE T80 are ~5 Å apart, and that will not change during the transport cycle (Fig. 2A). Likewise, Pro-78 in the MalG P1 loop will maintain a distance of 5 to 10 Å from MalE G13 (11). The substrate might reach the binding cleft of MalE by small conformational changes of thus-far-unidentified periplasmic loop regions (MalG P3 might be a candidate, as it reaches into the binding cleft after release of maltose [32]). Substrate-loaded MalE bound to MalFG and ATP-bound $MalK_2$ result in the closure of the transport channel on the cytosolic side and in its opening at the periplasmic face, thereby shifting MalE toward its open conformation. The substrate gets released and enters the pore by contacting a single substrate binding site exclusively found in MalF (32). At this stage, MalF S205 comes transiently within a distance of 10 to 25 Å from MalE T31 (32), concomitantly with the formation of a stable complex between MalE and the transporter. Hydrolysis of one ATP (as in the vanadate-trapped state) might push the substrate further into the pore. This step is accompanied by MalF T177 moving apart from MalE T31 (Fig. 2C). Hydrolysis of the second ATP would then bring the transporter back to the apo state, with MalFG open to the cytosolic side, allowing the release of the substrate, followed by dissociation of phosphate and ADP. The distance between MalF S205 and MalE T31 is reset to >25 Å (Fig. 2D). Rebinding of ATP would then restore the resting state.

Finally, and as already mentioned, the large enterobacterial MalF P2 loop is almost unique among bacterial maltose ABC transporters and is missing in homologous systems of archaebacteria. This might cast a shadow on the generality of our findings, assuming that ABC importers operate by the same mechanism. At present, however, the maltose ABC transporter represents the only system for which the wealth of structural and biochemical data enabled us to depict a transport model in some detail. It remains to be established whether binding protein-transporter interactions, as demonstrated here for the P2 loop, will be exerted similarly by the much shorter extracytoplasmic loop regions of TMDs from other importers.

ACKNOWLEDGMENTS

We thank Heidi Landmesser (Humboldt-Universität zu Berlin, Germany) for excellent technical assistance.

This work was supported by the Deutsche Forschungsgemeinschaft (SFB 449, TP B14; SCHN 274/9-3) and by a fellowship of the German National Academic Foundation (to M.G.).

REFERENCES

1. **Ames, G. F.-L., C. E. Liu, A. K. Joshi, and K. Nikaido.** 1996. Liganded and unliganded receptors interact with equal affinity with the membrane complex of periplasmic permeases, a subfamily of traffic ATPases. J. Biol. Chem. *271*:14264–14270.
2. **Austermuhle, M. L., J. A. Hall, C. S. Klug, and A. L. Davidson.** 2004. Maltose-binding protein is open in the catalytic transition state for ATP hydrolysis during maltose transport. J. Biol. Chem. **279:**28243–28250.
3. **Bakker, E. P., and L. L. Randall.** 1984. The requirement for energy during export of β-lactamase in *Escherichia coli* is fulfilled by the total protonmotive force. EMBO J. **3:**895–900.
4. **Bohl, E., H. A. Shuman, and W. Boos.** 1995. Mathematical treatment of the kinetics of binding protein dependent transport systems reveals that both the substrate loaded and unloaded binding proteins interact with the membrane components. J. Theor. Biol. **172:**83–94.
5. **Boos, W., and J. M. Lucht.** 1996. Periplasmic binding protein-dependent ABC transporters, p. 1175–1209. *In* F. C. Neidhardt et al. (ed.), *Escherichia coli* and *Salmonella*: cellular and molecular biology, 2nd ed. ASM Press, Washington, DC.
6. **Chen, J., G. Lu, J. Lin, A. L. Davidson, and F. A. Quiocho.** 2003. A tweezers-like motion of the ATP-binding cassette dimer in an ABC transport cycle. Mol. Cell **12:**651–661.
7. **Chen, J., S. Sharma, F. A. Quiocho, and A. L. Davidson.** 2001. Trapping the transition state of an ATP-binding cassette transporter: evidence for a concerted mechanism of maltose transport. Proc. Natl. Acad. Sci. USA **98:**1525–1530.
8. **Covitz, K.-M.Y., C. H. Panagiotidis, L.-I. Hor, M. Reyes, N. A. Treptow, and H. A. Shuman.** 1994. Mutations that alter the transmembrane signalling pathway in an ATP binding cassette (ABC) transporter. EMBO J. **13:**1752–1759.
9. **Dassa, E.** 2003. Phylogenetic and functional classification of ABC (ATP-binding cassette) systems, p. 3–35. *In* I. B. Holland et al. (ed.), ABC proteins: from bacteria to man. Academic Press, New York, NY.
10. **Daus, M. L., M. Grote, P. Müller, M. Doebber, A. Herrmann, H.-J. Steinhoff, E. Dassa, and E. Schneider.** 2007. ATP-driven MalK dimer closure and reopening and conformational changes of the 'EAA' motifs are crucial for function of the maltose ATP-binding cassette transporter ($MalFGK_2$). J. Biol. Chem. **282:**22387–22396.
11. **Daus, M. L., S. Berendt, S. Wuttge, and E. Schneider.** 2007. Maltose binding protein (MalE) interacts with periplasmic loops P2 and P1, respectively, of the MalFG subunits of the maltose ATP-binding cassette transporter ($MalFGK_2$) from *Escherichia coli*/*Salmonella* during the transport cycle. Mol. Microbiol. **66:**1107–1122.
12. **Daus, M. L., H. Landmesser, A. Schlosser, P. Müller, A. Herrmann, and E. Schneider.** 2006. ATP induces conformational changes of periplasmic loop regions of the maltose ATP-binding cassette transporter. J. Biol. Chem. **281:**3856–3865.
13. **Davidson, A. L., H. A. Shuman, and H. Nikaido.** 1992. Mechanism of maltose transport in *Escherichia coli*: transmembrane signaling by periplasmic binding proteins. Proc. Natl. Acad. Sci. USA **89:**2360–2364.
14. **Doeven, M. K., G. van den Bogaart, V. Krasnikov, and B. Poolman.** 2008. Probing receptor-translocator interactions in the oligopeptide ABC transporter by fluorescence correlation spectroscopy. Biophys. J. **94:**3956–3965.
15. **Ehrmann, M., R. Ehrle, E. Hofmann, W. Boos, and A. Schlösser.** 1998. The ABC maltose transporter. Mol. Microbiol. **29:**685–694.
16. **Grote, M., E. Bordignon, Y. Polyhach, G. Jeschke, H.-J. Steinhoff, and E. Schneider.** 2008. A comparative EPR study of the nucleotide-binding domains' catalytic cycle in the assembled maltose ABC-importer. Biophys. J. **95:**2924–2938.
17. **Higgins, C. F.** 1992. ABC transporters: from microorganisms to man. Annu. Rev. Cell Biol. **8:**67–113.
18. **Hollenstein, K., D. C. Frei, and K. P. Locher.** 2007. Structure of an ABC transporter in complex with its binding protein. Nature **446:**213–216.

19. **Hor, L.-I., and H. A. Shuman.** 1993. Genetic analysis of periplasmic binding protein dependent transport in *Escherichia coli*. Each lobe of maltose-binding protein interacts with a different subunit of the $MalFGK_2$ membrane transport complex. J. Mol. Biol. **233:**659–670.
20. **Hunke, S., M. Mourez, M. Jèhanno, E. Dassa, and E. Schneider.** 2000. ATP modulates subunit-subunit interactions in an ATP-binding cassette transporter ($MalFGK_2$) determined by site-directed chemical cross-linking. J. Biol. Chem. **275:**15526–15534.
21. **Landmesser, H., A. Stein, B. Blüschke, M. Brinkmann, S. Hunke, and E. Schneider.** 2002. Large-scale purification, dissociation and functional reassembly of the maltose ATP-binding cassette transporter ($MalFGK_2$) of *Salmonella typhimurium*. Biochim. Biophys. Acta **1565:**64–72.
22. **Loo, T. W., and D. M. Clarke.** 2001. Determining the dimensions of the drug-binding domain of human P-glycoprotein using thiol cross-linking compounds as molecular rulers. J. Biol. Chem. **276:**36877–36880.
23. **Lu, G., J. M. Westbrooks, A. L. Davidson, and J. Chen.** 2005. ATP hydrolysis is required to reset the ATP-binding cassette dimer into the resting-state conformation. Proc. Natl. Acad. Sci. USA **102:**17969–17974.
24. **Mannering, D. E., S. Sharma, and A. L. Davidson.** 2001. Demonstration of conformational changes associated with activation of the maltose transport complex. J. Biol. Chem. **276:**12362–12368.
25. **Manson, M. D., W. Boos, P. J. Bassford, Jr., and B. A. Rasmussen.** 1985. Dependence of maltose transport and chemotaxis on the amount of maltose-binding protein. J. Biol. Chem. **260:**9727–9733.
26. **Martinez, E., B. Bartolomé, and F. de la Cruz.** 1988. pACYC 184-derived cloning vectors containing the multiple cloning site and *lacZ*α reporter gene of pUC8/9 and pUC18/19. Gene **68:**159–162.
27. **Merino, G., W. Boos, H. A. Shuman, and E. Bohl.** 1995. The inhibition of maltose transport by the unliganded form of the maltose-binding protein of *Escherichia coli*: experimental findings and mathematical treatment. J. Theor. Biol. **177:**171–179.
28. **Miller, J. H.** 1972. Experiments in molecular genetics. Cold Spring Harbor Laboratory Press, Cold Spring Harbor, NY.
29. **Mourez, M., M. Hofnung, and E. Dassa.** 1997. Subunit interactions in ABC transporters: a conserved sequence in hydrophobic membrane proteins of periplasmic permease defines an important site of interactions with the ATPase subunit. EMBO J. **16:**3066–3077.
30. **Neuhard, J., and P. Nygaard.** 1987. Purines and pyrimidines, p. 445–473. *In* F. C. Neidhardt et al. (ed.), *Escherichia coli* and *Salmonella*: cellular and molecular biology, 2nd ed. ASM Press, Washington, DC.
31. **Nikaido, H.** 1994. Maltose transport system of Escherichia coli: an ABC-type transporter. FEBS Lett. **346:**55–58.
32. **Oldham, M. L., D. Khare, F. A. Quiocho, A. L. Davidson, and J. Chen.** 2007. Crystal structure of a catalytic intermediate of the maltose transporter. Nature **450:**515–521.
33. **Quiocho, F. A.** 1990. Atomic structures of periplasmic binding proteins and the high-affinity active transport systems in bacteria. Philos. Trans. R. Soc. Lond. B **326**(1236)**:**341–351.
34. **Schmitt, L., and R. Tampé.** 2002. Structure and mechanism of ABC transporters. Curr. Opin. Struct. Biol. **12:**754–760.
35. **Schneider, E., and S. Hunke.** 1998. ATP-binding-cassette (ABC) transport systems: functional and structural aspects of the ATP-hydrolyzing subunits/domains. FEMS Microbiol. Rev. **22:**1–20.
36. **Sharma, S., and A. L. Davidson.** 2000. Vanadate-induced trapping of nucleotides by purified maltose transport complex requires ATP hydrolysis. J. Bacteriol. **182:**6570–6576.
37. **Shilton, B. H.** 2008. The dynamics of the MBP-$MalFGK_2$ interaction: a prototype for binding protein dependent ABC-transport systems. Biochim. Biophys. Acta **1778:**1772–1780.
38. **Smith, P. C., N. Karpowich, L. Millen, J. E. Moody, J. Rosen, P. J. Thomas, and J. F. Hunt.** 2002. ATP binding to the motor domain from an ABC transporter drives formation of a nucleotide sandwich dimer. Mol. Cell **10:**139–149.
39. **Sun, J. Z., J. Voss, W. L. Hubbell, and H. R. Kaback.** 1999. Proximity between periplasmic loops in the lactose permease of *Escherichia coli* as determined by site-directed spin labeling. Biochemistry **38:**3100–3105.
40. **Szmelcman, S., N. Sassoon, and M. Hofnung.** 1997. Residues in the α helix 7 of the bacterial maltose binding protein which are important in interactions with the $MalFGK_2$ complex. Protein Sci. **6:**628–636.
41. **Tang, C., C. D. Schwieters, and G. M. Clore.** 2007. Open-to-close transition in apo maltose-binding protein observed by paramagnetic NMR. Nature **449:**1078–1082.
42. **Tapia, M. I., M. Mourez, M. Hofnung, and E. Dassa.** 1999. Structure-function study of MalF protein by random mutagenesis. J. Bacteriol. **181:**2267–2272.
43. **Zaitseva, J., S. Jenewein, T. Jumpertz, I. B. Holland, and L. Schmitt.** 2005. H662 is the linchpin of ATP hydrolysis in the nucleotide-binding domain of the ABC transporter HlyB. EMBO J. **24:**1901–1910.